

Research Paper

Functional role of BTB and CNC Homology 1 gene in pancreatic cancer and its association with survival in patients treated with gemcitabine

Xudong Huang^{1*}, Jian Zheng^{2*}, Jun Li^{1*}, Xu Che^{3*}, Wenle Tan¹, Wen Tan¹, Mingming Shao¹, Xinxin Cheng¹, Zhongli Du¹, Yanjie Zhao¹, Chengfeng Wang³, Chen Wu¹, Dongxin Lin¹

1. Department of Etiology and Carcinogenesis, National Cancer Center/Cancer Hospital, Chinese Academy of Medical Sciences and Peking Union Medical College, Beijing 100021, China
2. Sun Yat-sen University Cancer Center, State Key Laboratory of Oncology in South China and Collaborative Innovation Center for Cancer Medicine, Guangzhou 510060, China
3. Department of Abdominal Surgery, National Cancer Center/Cancer Hospital, Chinese Academy of Medical Sciences and Peking Union Medical College, Beijing 100021, China

*These authors contributed equally to this work.

✉ Corresponding authors: Dongxin Lin, Department of Etiology and Carcinogenesis, Cancer Hospital, Chinese Academy of Medical Sciences. Phone: 10-87788715; Fax: 10-67722460; Email: lindx@cicams.ac.cn; Chen Wu, Department of Etiology and Carcinogenesis, Cancer Hospital, Chinese Academy of Medical Sciences. Phone: 10-87787395; Fax: 10-67722460; Email: chenwu@cicams.ac.cn or Chengfeng Wang, Department of Abdominal Surgery, Cancer Hospital, Chinese Academy of Medical Sciences. Phone: 10-87788491; Email: wangcf369@medmail.com.cn.

© Ivyspring International Publisher. This is an open access article distributed under the terms of the Creative Commons Attribution (CC BY-NC) license (<https://creativecommons.org/licenses/by-nc/4.0/>). See <http://ivyspring.com/terms> for full terms and conditions.

Received: 2017.11.22; Accepted: 2018.03.27; Published: 2018.05.23

Abstract

Genetic variation (rs372883C/T) in the 3'-untranslated region of BTB and CNC homology 1 (*BACH1*) has been associated with pancreatic ductal adenocarcinoma (PDAC) risk in our previous genome-wide association study; however, the action roles of this genetic variation in PDAC remains unknown.

Methods: *BACH1* expression was measured by quantitative real-time PCR, Western blot and immunohistochemistry. The effects of *BACH1* on cell proliferation and sensitivity to gemcitabine were examined by alteration of *BACH1* expression in PDAC cells. Angiogenesis was determined in vitro using a human umbilical vein endothelial cell model. Reporter gene assays were conducted to compare the effects of microRNA-1257 on rs372883 variation. The associations between rs372883 variants and survival time in patients treated with gemcitabine were estimated by logistic regression.

Results: We found substantially lower *BACH1* expression in PDAC compared with normal pancreatic tissues and the rs372883T allele had significantly lower *BACH1* levels than the rs372883C allele in both tumor and normal tissues. Knockdown of *BACH1* expression provoked proliferation of PDAC cells and angiogenesis, which might result from upregulation of hemeoxygenase-1 that evokes oncogenic AKT and ERK signaling. The rs372883T>C change inhibits interaction of *BACH1* with microRNA-1257, resulting in increased *BACH1* expression. PDAC patients with the rs372883T allele were more resistant to gemcitabine and had shorter survival time compared with those with the rs372883C allele.

Conclusion: These results shed light on the mechanism underlying the associations of *BACH1* rs372883 variation with risk of developing PDAC and differential gemcitabine sensitivity in patients.

Key words: pancreatic cancer, *BACH1*, HO-1, genetic variation, survival

Introduction

The survival rate for pancreatic ductal adenocarcinoma (PDAC) is among the worst for any cancer due to the lack of effective means for screening and early diagnosis [1, 2]. Gemcitabine is the first line

chemotherapy given to patients with advanced or unresectable PDAC [3, 4] but response varies greatly. Accumulating evidence indicates that genetic factors may play important roles in tumorigenesis and

response to chemotherapy [5–7]. In recent years, efforts have been made to identify susceptibility loci associated with sporadic PDAC through genome-wide association studies (GWAS) [8–13], which have provided further understanding of the pathogenesis of the disease. However, clinical utilization of the GWAS findings as specific biomarkers for early detection and diagnosis remains limited, and one of the major obstructions is lack of a functional mechanism [14]. Thus, functional characterization of GWAS-identified genetic variants has a fundamental merit.

The strongest association signal in our previous GWAS of PDAC was rs372883T>C variation located in the 3'-untranslated region (3'UTR) of the BTB and CNC homology 1 gene (*BACH1*) on 21q21.3. The C allele was associated with significantly decreased PDAC risk compared with the T allele [11]. Nevertheless, the role of *BACH1* variant in the development of PDAC remains unclear. *BACH1*, ubiquitously expressed in various tissues [15–17], is a transcriptional repressor of *HMOX1* encoding heme oxygenase-1 (HO-1), a rate-limiting enzyme in heme catabolism. At low heme level, *BACH1* binds directly to the *HMOX1* enhancer and represses HO-1 expression; however, at high heme concentration, the bound *BACH1* is relieved, resulting in the upregulation of HO-1 [18]. HO-1 may also play important roles in other cellular processes such as oxidative stress, metabolic inflammation, cell cycle, apoptosis and angiogenesis [19–23]. Thus, disruption of feedback regulation in the *BACH1*/HO-1 pathway may be implicated not only in cancer development but also in the sensitivity of cancer cells to chemotherapeutic agents.

Since rs372883C>T variation located in the *BACH1* 3'UTR might disrupt the binding of certain regulatory microRNAs and thus affect *BACH1* expression, in this study, we performed functional analysis of rs372883 variants and examined the effects of altered *BACH1*/HO-1 signaling pathway on the phenotypes of PDAC cells. In addition, we investigated whether *BACH1* rs372883 variation is associated with response to gemcitabine chemotherapy and survival time in PDAC patients.

Methods

Study subjects

Subjects with PDAC (N=102) were recruited between November 2002 and December 2014 (Table S1). Among them, 82 were treated with gemcitabine alone while the other 20 were treated with gemcitabine after surgical resection at a dose of 1,000 mg/m² delivered on days 1, 8 and 15 every 28 days.

Responsiveness was evaluated with RECIST criteria [24] after accomplishing at least two courses of treatment. We defined patients achieving complete response (CR) or partial response (PR) as responders, and patients with stable disease (SD) or progressive disease (PD) as nonresponders. Survival time was measured from the date of diagnosis to the date of last follow-up or death. The last date of follow-up was 30th May 2015 and the median follow-up time was 33 months. Patients alive on the last follow-up date were considered censored. Twelve patients were lost to follow-up during this period and therefore only 90 patients were included in the survival analysis. Informed consent was obtained from all participants, and this study was approved by the Institutional Review Board of the Chinese Academy of Medical Sciences Cancer Hospital. All experiments on the participants in this study were performed in accordance with the relevant guidelines and regulations.

Analysis of *BACH1* genotypes

A blood DNA sample was obtained from each subject at the time of diagnosis and the *BACH1* rs372883 genotypes were determined using a TaqMan genotyping platform (ABI 7900HT system) with the primers and probes shown in Table S2.

In silico analysis of interaction between *BACH1* 3'UTR and microRNAs

We used publicly available software FINDTAR3 (<http://bio.sz.tsinghua.edu.cn/>), RegRNA (<http://regRNA.mbc.nctu.edu.tw/php/prediction.php>) and Snip Mir (<http://www.microarray.fr:8080/merge/index?action=MISNP>) to analyze the potential interactions between different *BACH1* 3'UTR sequences and microRNAs.

Cell lines and cell culture

Human PDAC cell lines CFPAC-1, BXPC-3 and Capan-2, human umbilical vein endothelial cell line HUVEC and human embryonic kidney cell line 293T were purchased from the China Infrastructure of Cell Line Resources (Beijing). Cells passaged for less than 6 months were authenticated by DNA fingerprinting analysis using short-tandem repeat (STR) markers.

Reporter gene construction and luciferase reporter assays

The full length of *BACH1* 3'UTR amplified from a rs372883TT homozygous DNA sample was subcloned into the psiCHECK-2 vector (Promega) and designated as p-T_{rs372883}, which was site-specifically mutated to create its variant counterparts p-C_{rs372883}. The constructs were transfected respectively into CFPAC-1 and BXPC-3 cells with or without miR-1257.

Renilla luciferase activity was detected with a Dual-Luciferase Reporter Assay System (Promega) and normalized using the firefly luciferase activity.

RNA preparation and quantitative real-time PCR (qRT-PCR) analysis

Total RNA was extracted from PDAC cell lines and surgically removed pancreatic specimens from 75 individuals. First-strand cDNA was synthesized by using the Superscript II-reverse transcriptase kit (Invitrogen). qRT-PCR was accomplished using the SYBR Green method on an ABI Prism 7900HT system.

Northern blot of microRNA

Total RNA extracted from CFPAC-1 and BXPC-3 cells was separated on denaturing polyacrylamide gels and transferred to Immobilon-Ny⁺ Membrane (Millipore, INYC00010). After pre-hybridization in DIG Easy Hyb buffer (Roche, 12039672910), the membrane was hybridized with the denatured 3'-digoxigenin-labeled complementary sequence of miR-1257 probe (Table S2) and detected using an Odyssey infrared scanner (Li-Cor, Lincoln).

Plasmids, lentiviral production and transduction

BACH1 cDNA made from CFPAC-1 cells was PCR-amplified and subcloned into pLvX-IRES-Neo vector (Clontech). Two short hairpin RNAs (shRNAs) were synthesized (GenePharma) for *BACH1* suppression (Table S2). They were respectively inserted into the pSIH1-H1-Puro lentiviral shRNA vector (System Biosciences) to produce lentivirus in 293T cells. CFPAC-1 and BXPC-3 cells were infected with concentrated virus. The supernatant was replaced with complete culture media after 24 h, followed by selection with G418 or puromycin, respectively.

Gene expression profiling, gene ontology and gene set enrichment analysis

Total RNA extracted from CFPAC-1 cells with or without *BACH1* knockdown were subject to analysis by the Agilent human lncRNA+mRNA array V.4.0 platform (Agilent Technologies). The raw and processed microarray data have been submitted to the Gene Expression Omnibus (accession number GSE111506). For Gene Ontology (GO) analysis, differentially expressed protein-coding genes were uploaded to online software DAVID (<http://david.abcc.ncifcrf.gov/>) and $P < 0.05$ was considered significant for the biological process enrichment. For Gene Set Enrichment Analysis (GSEA), gene profiling data were uploaded to GSEA 3.0. Hallmark gene sets were obtained from MSigDBv6.1 (<http://software.broadinstitute.org/gsea/msigdb/index.jsp>). False discov-

ery rate (FDR) < 0.25 was considered significant for enriched biological pathways.

Transient overexpression and RNA interference of *HMOX1*

Full length of *HMOX1* cDNA was PCR-amplified from total RNA isolated from CFPAC-1 cells and the fragment was subcloned into the pcDNA3.1 vector (Invitrogen). Small interfering RNA (siRNA) targeting *HMOX1* and its scramble control (Table S2) were obtained from GenePharma. Transfections were done with lipofectamine 2000.

Western blot assays

Total protein (60 μ g) extracted from cells or tissue samples was resolved by SDS-PAGE and transferred to PVDF membrane (Millipore). Antibody against BACH1 (A303-057A) was from Bethyl Laboratories while antibodies against other proteins were from Abcam (HO-1, ab52947; ERK1/2, ab36991; phosphorylated ERK1/2, ab76299; NRF2, ab62352; OCT4, ab181557; ABCG2, ab207732; ALDH1, ab52492 and TRA-1-60, ab16288), Santa-Cruz (HIF1A, sc-10790; VEGF, sc-152 and β -ACTIN, sc-47778) and Cell Signaling Technology (AKT, #9272; phospho-AKTThr308, #9275; phospho-AKTSer473, #9271; PTEN, #9559; eNOS, #9586; phospho-eNOSer1177, #9570; E-CADHERIN, #3195; VIMENTIN, #5741; ZO-1, #8193; ZEB1, #3396 and SLUG, #9585). The membranes were incubated with the primary antibody and visualized with a Phototope-horseradish peroxidase Western Blot Detection kit (Cell Signaling Technology).

Chromatin immunoprecipitation combined quantitative PCR (ChIP-qPCR)

CFPAC-1 and BXPC-3 cells were treated with formaldehyde for cross linking, followed by ChIP with antibody against BACH1 (Santa-Cruz, sc-14700X), NRF2 (Abcam, ab62352) or mouse IgG. The level of *HMOX1* was determined by qPCR using SYBR Green and the primers for *HMOX1* and its enhancer regions 1 and 2 [25, 26].

Cell viability and colony formation assays

Cell viability was measured using CCK-8 kit (Dojindo). Colony formation ability was determined by counting number of cells in 12-well cell-culture cluster with complete growth media after fixing with methanol and stained with crystal violet.

Enzyme-linked Immunosorbent assay (ELISA) of VEGF protein

CFPAC-1 and BXPC-3 cells with overexpression or knockdown of *BACH1* were cultured in a complete medium for 48h. The culture medium was collected

for ELISA of VEGF using the VEGF ELISA kit (R&D System).

In vitro angiogenesis assays

HUVECs were seeded at a density of 2×10^4 cells per well on growth factor-reduced Matrigel (Corning 356231) and grown in a conditioned medium collected from CFPAC-1 or BXPC-3 cells with overexpression or knockdown of *BACH1*. The morphologic change of HUVECs was photographed and tube formation was counted after cultivation for 6h.

Drug sensitivity assays

Cells in growth medium were exposed to various concentrations of gemcitabine (Selleck, S1714) and enumerated using CCK-8 kit at 48 h of exposure. Gemcitabine sensitivity was expressed as drug concentration that inhibits cell proliferation by 50% (IC_{50}).

Xenograft tumor formation assays

Five-week old female BALB/c nude mice (6 animals in each group) were subcutaneously injected with 0.1 mL of cell suspension containing 1×10^6 cells into the back flank. Animals were raised in the following six weeks and tumor volume was measured every other day and calculated by $\text{length} \times \text{width}^2 \times 0.5$. Sample size was not predetermined for these experiments. All experimenters were blinded to which cells were injected in the mice. All animal handling and experimental procedures were performed in accordance with the relevant institutional and national guidelines.

Immunohistochemical (IHC) analysis

Tissue microarrays of PDAC and paired normal tissues (N=67) were incubated with the mouse anti-BACH1 antibody (1:100; Abcam, ab128486) and detected with the ABC kit (Pierce). The BACH1 labeling index was ranked according to the percentage of positive cell nuclei and staining scores were calculated using an immunoreactive scoring (IRS). BACH1 labeling score of intensity was estimated as negative (0), weak (1), moderate (2) and strong (3). The extent of staining, defined as the percentage of positive staining cells, was scored as 1 ($\leq 10\%$), 2 (11%–50%), 3 (51%–75%) and 4 ($>75\%$). The total IRS was obtained by multiplying the score of intensity and that of extent, ranking from negative to >6 (+++). Owing to limited sample size, IRS was categorized into weak expression group ($IRS < 4$) and strong expression group ($IRS \geq 4$).

Statistical analysis

The statistical significance of comparison between two groups was determined using Student's

t-test. Wilcoxon matched-pairs test was used to assess IHC IRS score within cancer and matched normal tissues. Odds ratios (ORs) and their 95% confidence intervals (CIs) were calculated using logistic regression model adjusting for sex, age, tumor stage and surgery. Hazard ratios (HRs) and their 95% CIs were calculated using Cox proportional hazard models and adjusted for covariates that might influence the length of survival, including sex, age, tumor stage and surgery. Kaplan-Meier survival estimates were plotted, and the significances were assessed using log-rank tests. All statistical analyses were performed using SPSS (version 20.0, SPSS Inc.). $P < 0.05$ was considered statistically significant.

Results

BACH1 is downregulated in PDAC

We first examined the expression status of *BACH1* in PDAC and normal tissues and found that 76.0% (57/75) of tumors expressed significantly lower *BACH1* mRNA than their adjacent normal tissues ($P < 0.0001$; **Figure 1A**). Western blot analysis of randomly selected 35 pairs of samples showed that 23 (65.7%) had lower *BACH1* protein levels in tumors than in normal tissues (**Figure 1B**). IHC staining of *BACH1* on tissue microarrays revealed strong signals in both cytoplasm and nuclei of normal pancreatic duct cells and acinar cells; however, *BACH1* staining was apparently reduced in tumors (**Figure 1C**). Two published data sets [27, 28] also showed significantly lower *BACH1* mRNA in PDAC than in normal tissues (**Figures 1D–E**), consistent with our results.

BACH1 inhibits in vitro PDAC cell proliferation and angiogenesis

To explore the whole landscape of gene expression programs regulated by *BACH1* in PDAC, we performed gene expression profile analysis in CFPAC-1 cells with or without *BACH1* knockdown. Gene ontology analysis showed that differentially expressed genes were enriched in many pathways including transcription, redox process, RAS signal transduction, cell proliferation, stem cell maintenance, cell migration, vascular endothelial growth factor receptor signaling pathway, apoptotic process and positive regulation of epithelial to mesenchymal transition (**Figure S1A**). Gene set enrichment analysis revealed that genes upregulated in CFPAC-1 cells with *BACH1* knockdown were enriched in ROS pathway, glycolysis, angiogenesis, complement, xenobiotic metabolism, MTORC1 signaling, hypoxia, MYC targets, P53 pathway and epithelial-mesenchymal transition (**Figure S1B** and **Table S3**). Based on these findings, we next examined the impact

of *BACH1* on PDAC cell proliferation by altering *BACH1* expression in CFPAC-1 and BXPC-3 cells (**Figure 2A**). Overexpression of *BACH1* substantially inhibited colony formation (**Figure 2B**) and cell proliferation (**Figure 2C**) while knockdown of *BACH1* expression accelerated colony formation and proliferation abilities of cells (**Figures 2B and 2D**). The inhibitory effect of *BACH1* on PDAC cell proliferation was also replicated in vivo by xenograft growth in mice (**Figures 2E–F**). To explore the effect of *BACH1* on angiogenesis, we first examined the VEGF levels secreted by CFPAC-1 and BXPC-3 cells in the culture

medium and the results showed that overexpression of *BACH1* significantly suppressed VEGF levels in the supernatant but knockdown of *BACH1* expression significantly elevated the levels (**Figure 2G**). In vitro angiogenesis assays using HUVEC model showed that tube formation was greatly enhanced by culture with the supernatants from PDAC cells having *BACH1* knockdown compared with that by culture with the supernatants from cells having *BACH1* overexpression (**Figure 2H**).

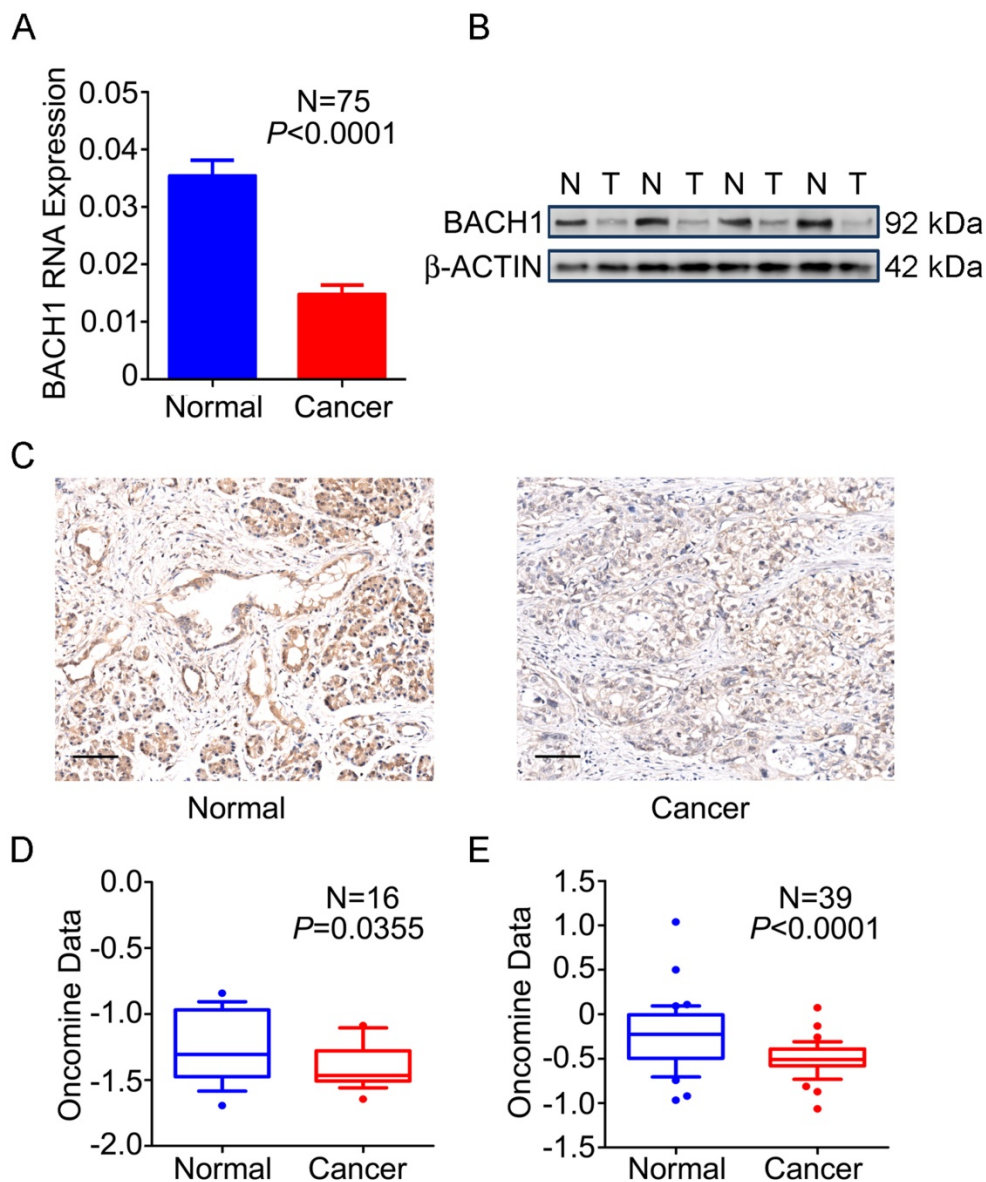


Figure 1. Expression of *BACH1* in PDAC. (A) *BACH1* mRNA levels determined by qRT-PCR were significantly lower in PDAC compared with paired adjacent normal tissues (N=75). Results represent mean \pm SEM normalized to *GAPDH* and *P*-values are for Student's *t*-test. (B) *BACH1* protein levels determined by Western blot were significantly lower in PDAC (T) than in paired normal tissues (N). Shown is a representative picture selected from 35 pairs of clinical specimens. (C) Representative IHC images (200 \times) showing *BACH1* protein expression in normal pancreatic tissues (left) and PDAC (right). Bar scale, 100 μ m. (D–E) Expression of *BACH1* in published data sets of Pei et al.[27] and Badea et al. [28] (Oncomine, <https://www.oncomine.org/resource/main.html>). The line in the middle of the box represents the median; bars represent 10th and 90th percentiles and greater values were plotted as individual points. *P*-values are for unpaired Wilcoxon rank-sum test.

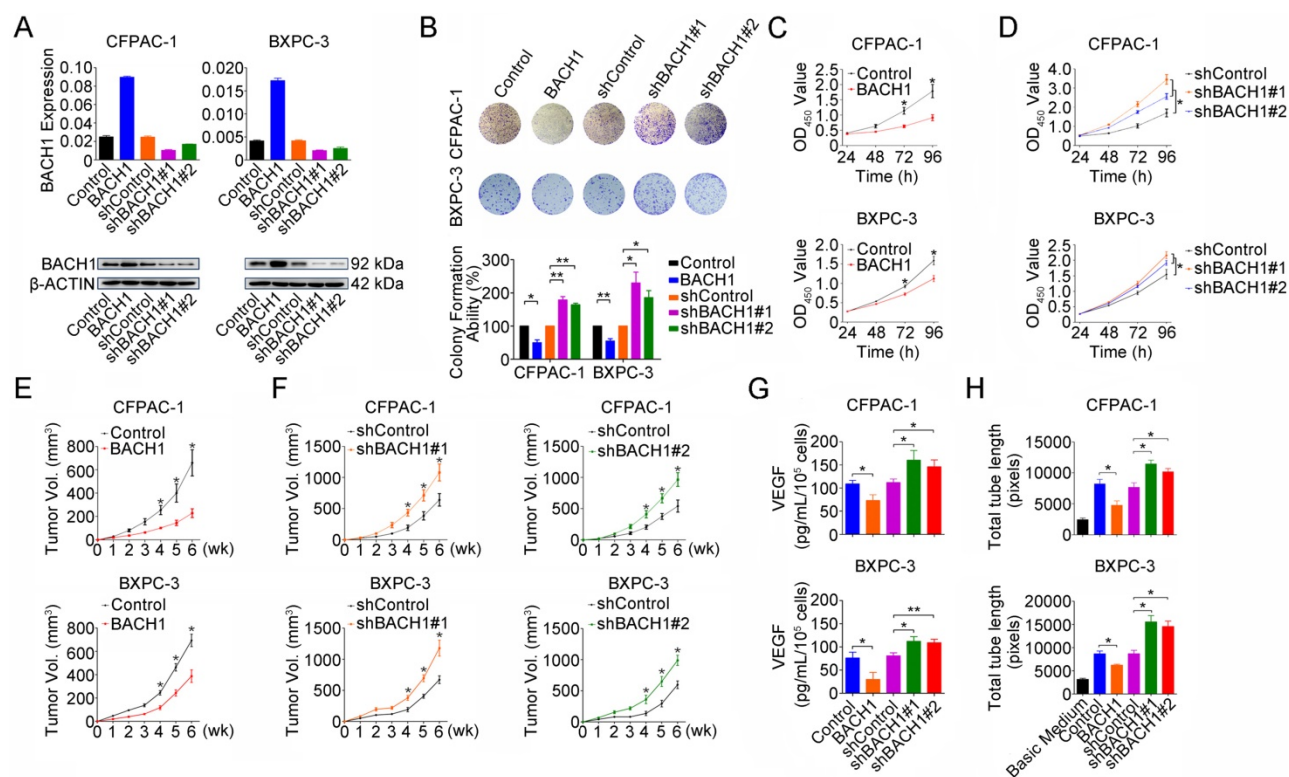


Figure 2. *BACH1* inhibits PDAC cells proliferation and angiogenesis. (A) Stable overexpression or knockdown of *BACH1* in CFPAC-1 and BXPC-3 cells. **(B)** Effect of *BACH1* overexpression or knockdown on colony formation of CFPAC-1 and BXPC-3 cells. Results represent colony formation ability relative to Control or shControl set to 100% from three experiments. *P*-values are for Student's *t*-test. *, *P*<0.05; **, *P*<0.01 compared with Control or shControl. **(C)** Overexpression of *BACH1* substantially reduced proliferation of both CFPAC-1 and BXPC-3 cells determined by CCK-8 assay. Results are mean ± SEM from three experiments and each experiment had six replicates. *, *P*<0.05 compared with control. **(D)** Knockdown of *BACH1* significantly enhanced proliferation of both CFPAC-1 and BXPC-3 cells. Results are mean ± SEM from three experiments and each experiment had six replicates. *, *P*<0.05 compared with shControl. **(E–F)** Xenograft tumor formation and growth of CFPAC-1 and BXPC-3 cells with *BACH1* overexpression or knockdown in nude mice. Results are mean ± SEM from 6 animals in each group. *, *P*<0.05 compared with Control or shControl. **(G)** Effect of *BACH1* expression on VEGF levels quantified by ELISA in the culture medium of CFPAC-1 or BXPC-3 cells. Results are mean ± SEM from three measurements. *, *P*<0.05; **, *P*<0.01 compared with Control or shControl. **(H)** Effects of culture medium of CFPAC-1 or BXPC-3 cells with *BACH1* overexpression or knockdown on HUVEC tube formation. Results are mean ± SEM from three measurements. *, *P*<0.05 compared with Control or shControl.

BACH1 negatively regulates HO-1 expression

To shed light on the underlying molecular mechanism that *BACH1* may act, we combined published *BACH1* ChIP-sequencing data (GEO accession: GSM693953 and GSM693952) [29] and differentially expressed genes (fold change>1.5 or <-1.5) identified by our microarray analysis. We found 8 genes that were directly regulated by *BACH1* and, among them, *HMOX1* was the mostly upregulated one (Figure 3A and Figure S2). We confirmed that *BACH1* can bind to the *HMOX1* enhancers [29] (Figures 3B–C) and overexpression of *BACH1* substantially suppressed HO-1 expression while knockdown of *BACH1* substantially increased HO-1 expression in PDAC cell lines (Figure 3D). Furthermore, we found that *HMOX1* levels were significantly higher in PDAC than in normal pancreatic tissues (*P*<0.0001; Figure 3E) and were negatively correlated with *BACH1* levels (Figures 3F–H). *NRF2* is thought to be a transactivator in *NRF2*/*BACH1* transcriptional network. However, we

found that the change of *BACH1* expression had no effect on *NRF2* expression at both mRNA and protein levels (Figure S3A). ChIP-qPCR assays showed that *NRF2* can also bind to the *HMOX1* enhancers. However, when *BACH1* was overexpressed in cells, less *NRF2* was enriched in EN1 and EN2; in contrast, when *BACH1* expression was knocked down, more *NRF2* was enriched in EN1 and EN2 (Figure S3B).

BACH1 controls cell proliferation and angiogenesis via regulating HO-1 expression

We further examined the impact of HO-1 on PDAC cell proliferation under the *BACH1* overexpression or knockdown condition. When *BACH1* was overexpressed in CFPAC-1 and BXPC-3 cells, HO-1 was substantially reduced; however, forced restoration of HO-1 expression in cells efficiently overcame the repression of cell proliferation and colony formation caused by overexpression of *BACH1* (Figures S4A–B). In contrast, silencing HO-1 expression successfully suppressed proliferation and colony formation caused by knockdown of *BACH1*

expression in the same cells (Figures S4C–D). These results suggest that the effect of *BACH1* on cell proliferation is largely mediated by HO-1. We then examined the changes of molecules downstream HO-1 focusing on aberrant activation and regulation of AKT, ERK, eNOS, HIF1A, PTEN and VEGF, which has been well-known to be involved in cancer cell proliferation and angiogenesis [30–33]. We found that when *BACH1* was overexpressed in CFPAC-1 and BXPC-3 cells, HO-1 and phosphorylated AKT, eNOS and ERK1/2 were substantially reduced, although the total amount of AKT, eNOS and ERK1/2 were not significantly changed (Figure 4A). In addition, we also observed substantially decreased expression of *HIF1A* and *VEGF* and increased expression of *PTEN* in cells overexpressing *BACH1* (Figure 4A and Figure S5). These changes caused by alterations of *BACH1* expression could be rescued when HO-1 expression was restored (Figures 4A–B). In line with these results in vitro in cells, we detected a reverse correlation between *BACH1* and *HIF1A* (Figure 4C) or *VEGF* (Figure 4D) mRNA expression and a positive correlation between *BACH1* and *PTEN* mRNA expression (Figure 4E) in both clinical PDAC and normal pancreatic tissues.

***BACH1* 3'UTR-rs372883T variant is a target of miR-1257**

To elucidate the effect of the rs372883T>C change on *BACH1* expression, we carried out reporter gene assays in CFPAC-1 and BXPC-3 cells. The results showed that the plasmid constructs containing the *BACH1* 3'UTR-rs372883T had significantly decreased luciferase expression compared with the *BACH1* 3'UTR-rs372883C counterparts (Figure 5A), suggesting that the rs372883T>C change may be a functional variation. In silico analysis showed that rs372883 lies within a binding site for the seed region of miR-1257 (MI0006391), the microRNA first described by Morin et al [34] and confirmed by Northern blot analysis in the present study (Figure S6). rs372883T>C change causes a base pair mismatch between miR-1257 and the *BACH1* 3'UTR (Figure 5B). The expression of reporter vectors p-T_{rs372883} and p-C_{rs372883} were then compared in PDAC cells in the presence of exogenous miR-1257 and the results showed that although miR-1257 had no effect on the expression of vector containing the *BACH1* 3'UTR-rs372883C (p-C_{rs372883}), it significantly suppressed the expression of vector containing the *BACH1* 3'UTR-rs372883T (p-T_{rs372883}). The suppressive effect of miR-1257 was in a dose-dependent manner and could be restored by co-transfection of the miR-1257 inhibitor (Figure 5C).

We then evaluated the association between rs372883 genotypes and *BACH1* mRNA levels in

clinical normal pancreatic tissues (N=75) and found that the *BACH1* mRNA levels were significantly lower in the rs372883 TT or CT genotype than that in the CC genotype (Figure 5D). However, these genotype-associated differences were not related to the miR-1257 levels because no significant differences in miR-1257 expression were observed among individuals (Figure 5E). As expected, *HMOX1* mRNA levels were significantly higher in the *BACH1* rs372883TT or CT genotype compared with that in the CC genotype (Figure 5F). These results suggest that rs372883T>C change may diminish the interaction between *BACH1* 3'UTR and miR-1257, enhancing *BACH1* expression which further negatively regulates HO-1 expression in a *BACH1* variant-dependent manner. Western blot analysis showed that PDAC specimens with the rs372883TT genotype had substantially lower *BACH1* protein levels but substantially elevated levels of activated signaling molecules that are critical in cell proliferation and angiogenesis such as phosphorylated-AKT, -ERK, -eNOS, *HIF1A* and *VEGF* compared with those with the rs372883CC genotype except for *PTEN*, which was substantially lower in the TT or CT genotype compared with the CC genotype (Figure 5G).

Sensitivity to gemcitabine in PDAC cells depends on *BACH1* in an allele-specific manner

Since response to gemcitabine varies greatly among patients, we performed drug sensitivity assays in PDAC cells by altering *BACH1* expression. We found that compared with vector controls, overexpression of *BACH1* significantly increased the sensitivity of both CFPAC-1 and BXPC-3 cells to gemcitabine but knockdown of *BACH1* substantially decreased the sensitivity (Figure 6A). Because *BACH1* is a suppressor for HO-1 expression, we thus investigated whether *BACH1*-dependent gemcitabine sensitivity is mediated by HO-1. We found that restoration of HO-1 expression in both CFPAC-1 and BXPC-3 cells overexpressing *BACH1* partially suppressed the sensitivity (Figure 6B), but silencing HO-1 expression in cells with knockdown of *BACH1* partially increased the sensitivity (Figure 6C).

We then looked at the effects of different rs372883 genotypes on gemcitabine sensitivity and found that in the absence of miR-1257, BXPC-3 cells carrying the rs372883CC genotype had an IC₅₀ that is significantly lower than CFPAC-1 cells carrying the rs372883CT genotype and Capan-2 cells carrying the rs372883TT genotype (Figures 6D–F). The presence of miR-1257 in the assay system significantly increased IC₅₀ for Capan-2 ($P=0.0390$) and CFPAC-1 ($P=0.0006$) but not for BXPC-3 ($P>0.05$) cells, with the fold-change being 7.32, 4.06 and 1.92, respectively

(Figures 6D–F and Figure S7), indicating a *BACH1* allele-dependent effect of miR-1257. Furthermore, the effect of miR-1257 on gemcitabine resistance in PDAC cells could be restored by co-transfection with the miR-1257 inhibitor (Figures 6D–F).

To further elucidate the mechanism for the gemcitabine sensitivity dependent on *BACH1* allele, we examined expressions of some drug-resistant genes including *ABCC2*, *MGST1* and *NQO1* in PDAC cells and found that in the presence of miR-1257, the expression of *ABCC2* ($P=0.0005$ and $P=0.0019$), *MGST1* ($P=0.0002$ and $P<0.0001$) and *NQO1* ($P=0.0002$ and $P=0.0048$) significantly increased in Capan-2 and CFPAC-1 cells but not in BXP-3 cells (all $P>0.05$; Figures S8A–C). Furthermore, the effect of miR-1257 on the expression of these drug-resistant genes in PDAC cells could be restored by co-transfection with the miR-1257 inhibitor (Figure S8A–C).

BACH1 regulates expression of genes involved in EMT and stemness

GO and GSEA results suggested that *BACH1*

may be involved in regulating EMT and cell pluripotency processes (Figures S1A–B and Table S3). We then examined the alteration of EMT associated markers in cells with *BACH1* overexpression or downregulation and found that when *BACH1* was overexpressed in CFPAC-1 and BXP-3 cells, the levels of *E-cadherin* and *ZO-1* were substantially increased but mesenchymal markers *ZEB1*, *Vimentin* and *Slug* were substantially reduced. The reverse results were observed in the same cells with *BACH1* knockdown (Figure S9A). In addition, we found that stemness markers *ABCG2* and *ALDH1* were substantially reduced when *BACH1* was overexpressed, but substantially increased when *BACH1* was knocked down (Figure S9B). However, we did not observe any changes of *OCT4*; *TRA-1-60* was not detectable in both cell lines (Figure S9B). By analyzing previously published results, we observed that the expression levels of *BACH1* were negatively correlated with *ABCG2* and *CXCR4* levels (Figure S9C–D).

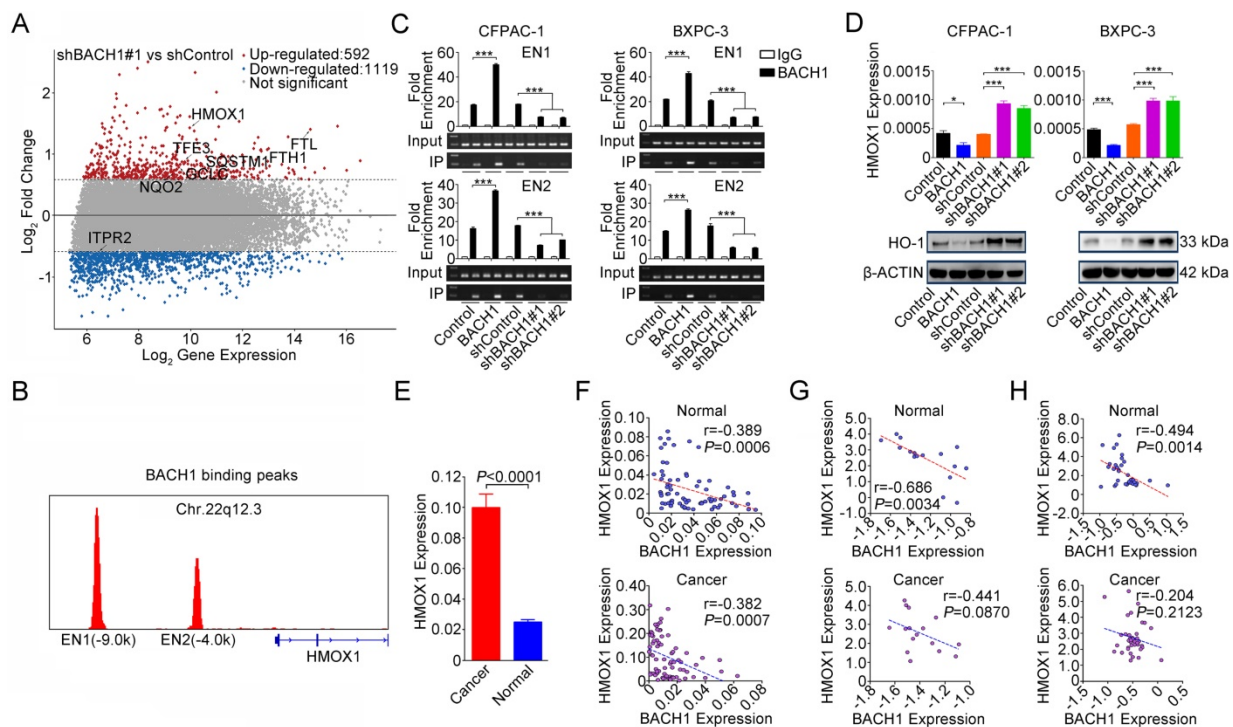


Figure 3. *BACH1* negatively regulates *HO-1* expression in PDAC cells. (A) MA plot of the gene expression profile. Eight genes directly regulated by *BACH1* were marked: red, upregulated; blue, downregulated; gray, not significantly changed. The dotted lines indicate the cut-off value of log₂ fold change (± 0.58). **(B)** *BACH1* binding peaks in the *HMOX1* gene locus based on ChIP-sequencing data (GSM693953 and GSM693952). **(C)** Chromatin immunoprecipitation assays showing binding of *BACH1* to two enhancers EN1 (–9.0kb) and EN2 (–4.0kb) in the upstream of *HMOX1* in CFPAC-1 and BXP-3 cells. Overexpression of *BACH1* in these cells substantially enhanced enrichment of *BACH1* in EN1 and EN2, while knockdown of *BACH1* substantially decreased the enrichment in these two enhancers. Fold enrichment (mean \pm SEM) represents DNA levels associated with *BACH1* or IgG relative to an input control from three independent experiments. IgG served as negative control. $***, P<0.001$ compared with Control or shControl. **(D)** Overexpression of *BACH1* suppressed *HO-1* expression while knockdown of *BACH1* elevated *HO-1* expression in both mRNA and protein levels in CFPAC-1 and BXP-3 cells. $* P<0.05$; $***, P<0.001$ compared with Control or shControl. **(E)** *HMOX1* mRNA expression was significantly higher in PDAC compared with their adjacent normal tissues (N=75). Results are mean \pm SEM normalized to *GAPDH* and the *P*-values are for Student's *t*-test. **(F)** Correlation between *BACH1* and *HMOX1* mRNA levels in PDAC and paired normal tissues (N=75). The RNA levels were determined by qRT-PCR and expressed relative to *GAPDH*. The *r*- and *P*-values are for Pearson's correlation analysis. **(G–H)** Correlation between *BACH1* and *HMOX1* mRNA levels in PDAC and paired normal tissues. Data are from Oncomine database generated by Pei et al. [27] and Badea et al. [28].

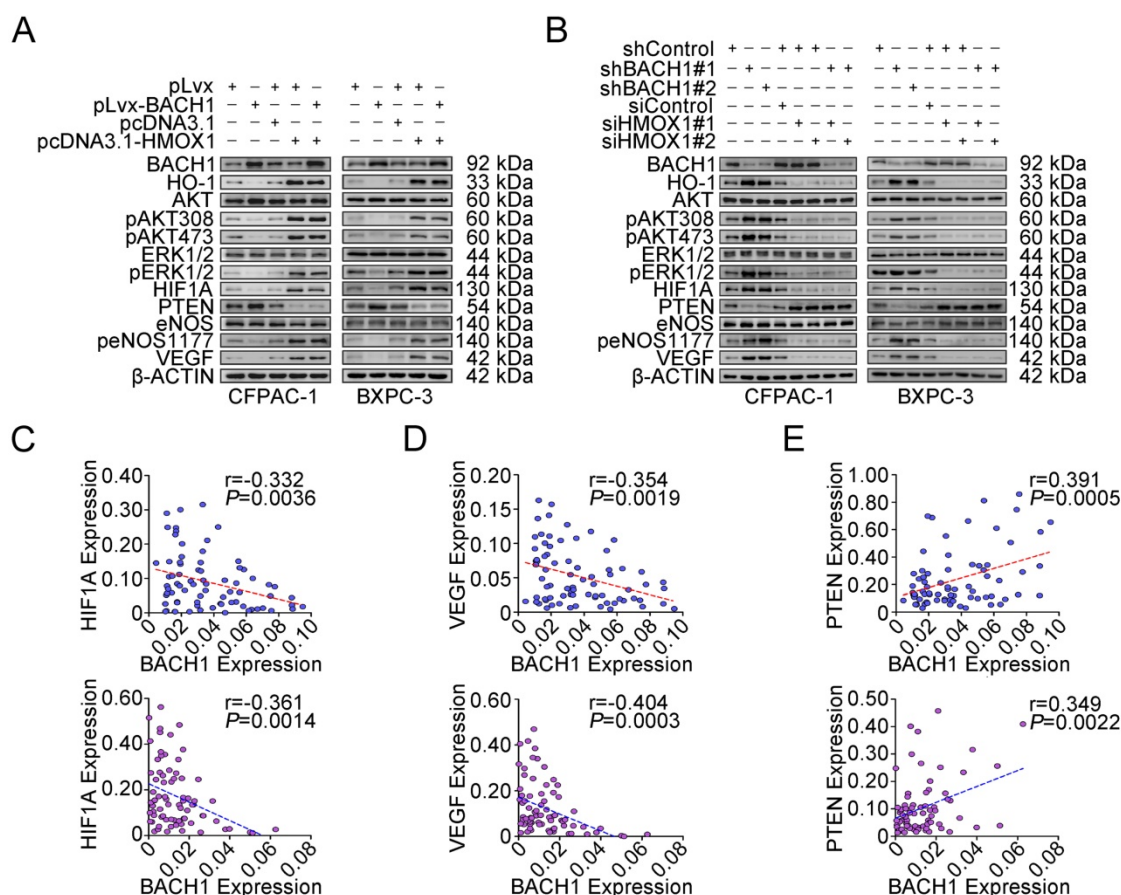


Figure 4. *BACH1* regulates signaling pathway downstream of HO-1. (A–B) Western blot analysis of AKT and ERK signaling modules downstream of HO-1 in CFPAC-1 and BXPc-3 cells with overexpression or knockdown of *BACH1*. (C–E) A reverse correlation between mRNA levels (N=75) of *BACH1* and mRNA levels of *HIF1A* (C) or *VEGF* (D) and a positive correlation between mRNA levels of *BACH1* and mRNA levels of *PTEN* (E) in normal tissues (upper panel) and paired PDAC (lower panel). The RNA levels were determined by qRT-PCR relative to *GAPDH*. The *r*- and *P*-values are for Pearson’s correlation analysis.

***BACH1* genotypes may predict gemcitabine response and prognosis in PDAC patients**

In 102 patients treated with gemcitabine, we observed a response rate of 15.7% and this was not related to the select clinical characteristics such as sex, age, tumor stage and surgery. The *BACH1* rs372883 genotypes appeared to have an ability to identify responsiveness: among responders, 37.5% of individuals carried the CC genotype, while among nonresponders, only 11.6% of individuals carried the CC genotype ($P=0.024$). The adjusted odds ratio of the CC genotype for being nonresponders was 0.15 (95% CI, 0.03–0.68) compared with the TT genotype (Table 1). However, there was no significant difference for the heterozygous CT genotype in responders and nonresponders (37.5% versus 46.5%, $P=0.745$). In this set of patients, 85 (83.3%) had died before the last follow-up time and the median survival time (MST) was 9.3 months. We observed significantly different survival times by tumor stage, with the MST being 14.4, 10.0 and 7.8 months for patients with local, locally advanced and metastatic tumor, respectively

($P_{\log\text{-rank}}=0.006$; Figure 7A). Patients who responded to gemcitabine also had longer MST than those who did not respond to the regimen (12.3 versus 8.2 months; Figure 7B) although the difference did not reach statistical significance ($P_{\log\text{-rank}}=0.175$) probably due to limited sample size. We then evaluated the association between *BACH1* rs372883 genotypes and PDAC survival time and found that the MST for the rs372883CC, CT and TT genotypes was 11.3, 9.8 and 7.5 months ($P_{\log\text{-rank}}=0.039$; Figure 7C). The per-allele hazard ratio for PDAC death was 0.63 (95% CI, 0.44–0.90; $P=0.01$).

Table 1. Response to gemcitabine therapy in patients with PDAC by *BACH1* rs372883 genotypes

Genotype	Responders*	Nonresponders*	OR (95% CI)§	P
TT	4 (25.0)	36 (41.9)	1.00 (Reference)	
CT	6 (37.5)	40 (46.5)	0.63 (0.15–2.57)	0.514
CC	6 (37.5)	10 (11.6)	0.15 (0.03–0.68)	0.014

*Responders include complete response and partial response while nonresponders include stable disease and progressive disease.

§OR, odds ratio, was calculated by logistic regression with adjustment for sex, age, tumor stage and surgery.

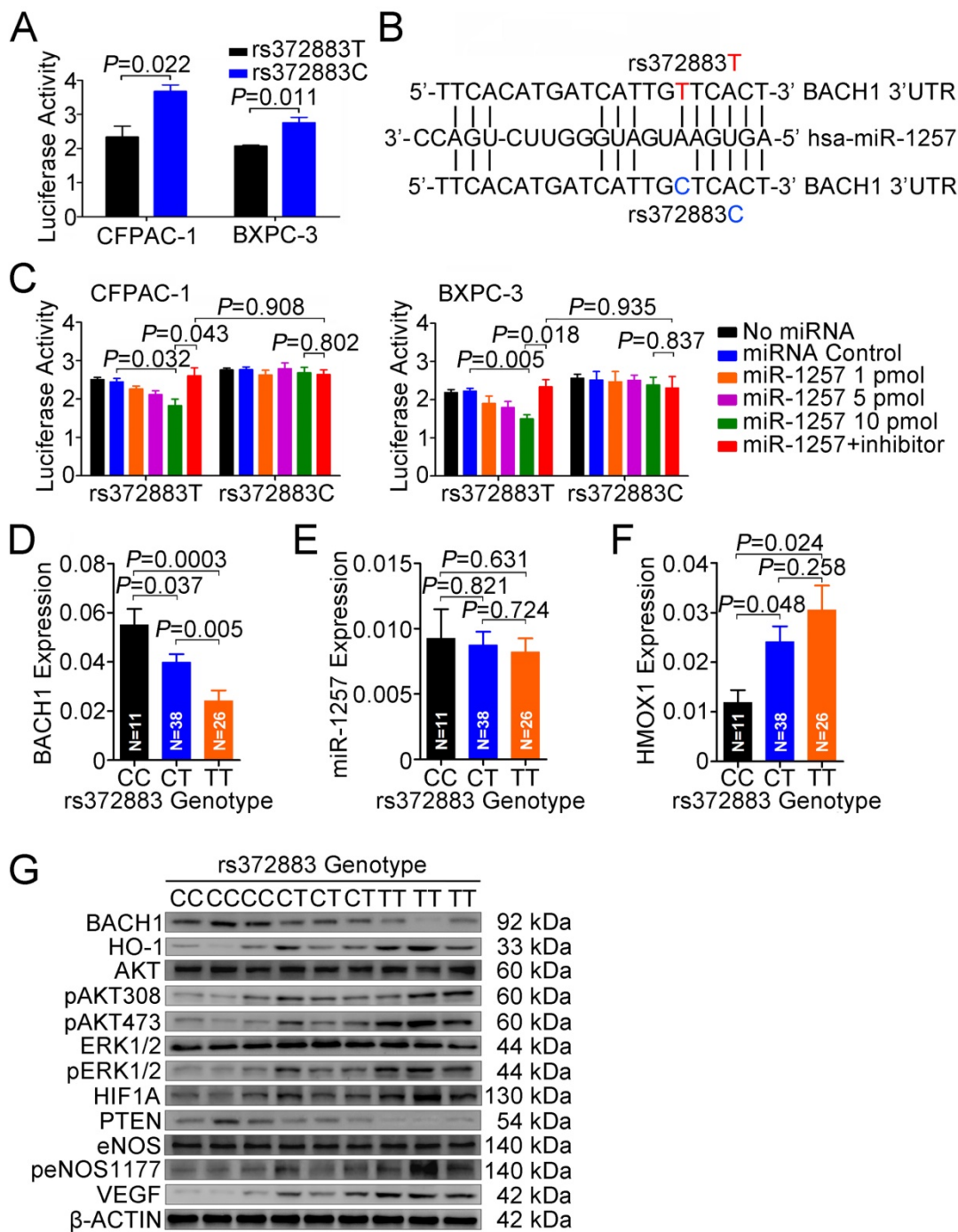


Figure 5. Functional relevance of rs372883 variants. (A) Relative reporter gene activity bearing *BACH1* 3'UTR fragment with the rs372883T or rs372883C allele in CFPAC-1 and BXPC-3 cells. Results are mean ± SEM from three experiments and each had six replicates. The P-values are for Student's t-test. (B) In silico prediction of interaction between miR-1257 and *BACH1* 3'UTR showing differences in binding within the seed region. (C) Relative reporter gene activity of the psiCHECK2-rs372883T and psiCHECK2-rs372883C constructs cotransfected with 1.0, 5.0 and 10.0 pmol of miR-1257 or its inhibitor in CFPAC-1 and BXPC-3 cells. Results are mean ± SEM from three experiments and each had six replicates; P-values were for Student's t-test. (D-F) Levels of *BACH1* mRNA, miR-1257 and *HMOX1* mRNA in normal pancreatic tissues adjacent to tumors of subjects with the rs372883 CC (N=11), CT (N=38) or TT (N=26) genotype. Results are mean ± SEM relative to *GAPDH* or *U6*. (G) Western blot analysis of AKT and ERK signaling modules downstream of HO-1 in surgically removed PDAC specimens from subjects with the rs372883CC, CT or TT genotype.

Discussion

In the previous GWAS, we identified rs372883 variant in *BACH1* 3'UTR as a genetic susceptibility locus for the development of PDAC [11]. The aim of the present study was to elucidate the functional

effect of this 3'UTR variant on *BACH1* expression and its consequential molecular role in PDAC. We demonstrate that *BACH1* is low-expressed in PDAC and knockdown of *BACH1* in PDAC cells provokes AKT and ERK oncogenic signaling via upregulation of HO-1 and thus promotes cell proliferation and

angiogenesis. Importantly, we found that rs372883 variant in *BACH1* 3'UTR lies on a binding site for miR-1257; the T>C change might diminish miR-1257 binding, resulting in a higher expression of *BACH1*. These experimental findings are consistent with our GWAS results and indicate that higher expression of *BACH1* rs372883C allele may be the underlying mechanism for reduced risk of PDAC in individuals carrying this variant. The supportive evidence for tumor suppressor role of *BACH1* in PDAC is also seen in TCGA database (<http://www.cbioportal.org/>

index.do), showing high frequencies of somatic mutations and copy number loss in the *BACH1* locus. However, we notice that some sets of *BACH1* mRNA profiling data from human PDAC in Oncomine database are not in line with our results, which is probably due to use of unpaired samples in these studies. In addition, in the present study, we have extended the results to the potential clinical implication that *BACH1* genotype may be a useful biomarker for the identification of gemcitabine treatment efficacy and prognosis of PDAC.

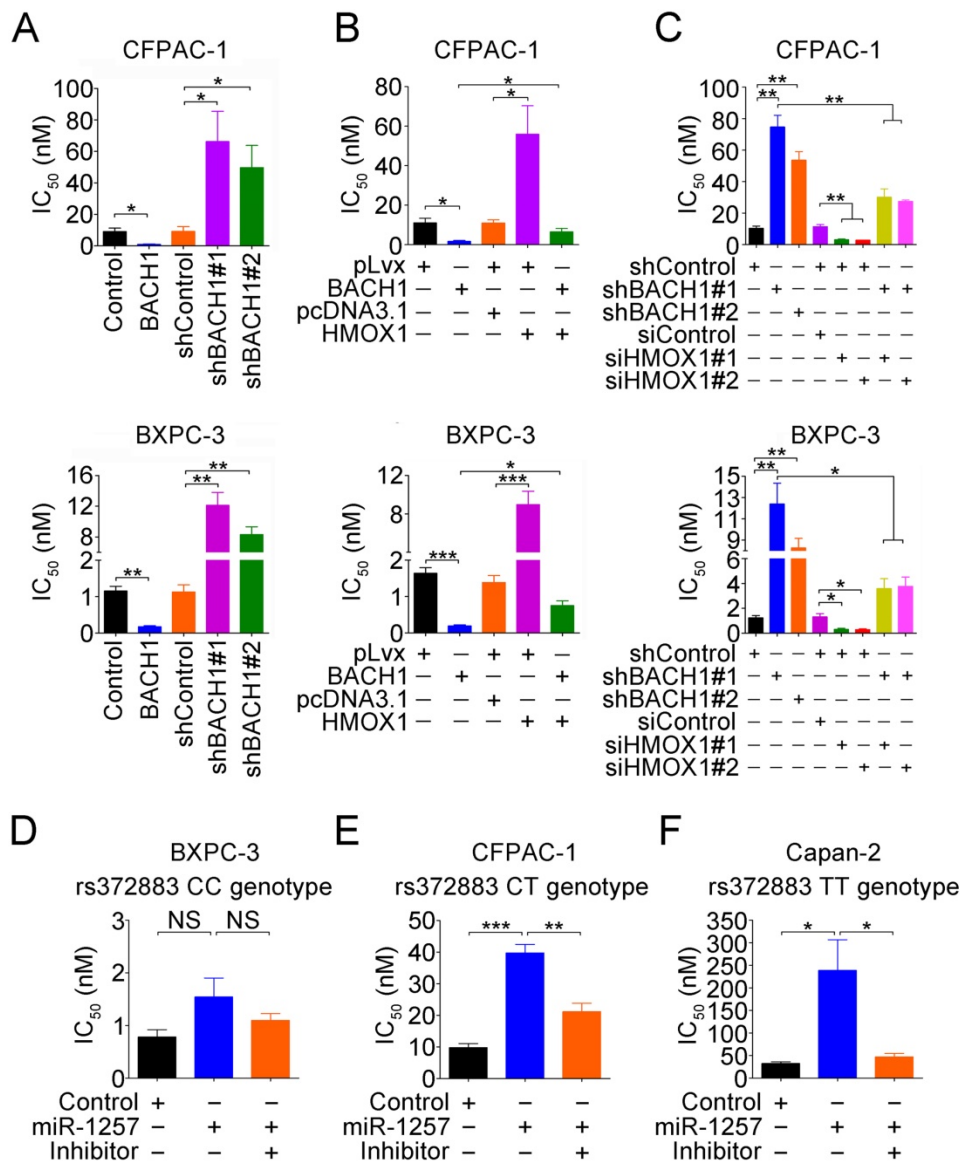


Figure 6. Gemcitabine sensitivity in PDAC cells depends on *BACH1* in an allele-specific manner. (A) Effects of *BACH1* on gemcitabine sensitivity in CFPAC-1 and BXPC-3 cells. Results represent mean ± SEM from three independent experiments and each had four replications. *, P<0.05 and **, P<0.01. (B–C) Effect of HO-1 expression on gemcitabine sensitivity in CFPAC-1 and BXPC-3 cells with overexpression (B) or knockdown (C) of *BACH1*. Results are mean ± SEM from three independent experiments and each had four replications. *, P<0.05; **, P<0.01 and ***, P<0.001. (D–F) Effect of miR-1257 on gemcitabine sensitivity in BXPC-3 (D), CFPAC-1 (E) and Capan-2 (F) cells carrying the rs372883 CC, CT or TT genotype, respectively. Cells transiently transfected with miR-1257 or its inhibitor were exposed to gemcitabine at final concentrations ranging from 10⁻³ to 10³ nM. Cells were enumerated with the CCK-8 assay at 48h after drug exposure. IC₅₀ represents gemcitabine concentration that inhibits cell proliferation by 50%. Results are mean ± SEM from three experiments and each had four replicates. *, P<0.05 and ***, P<0.001.

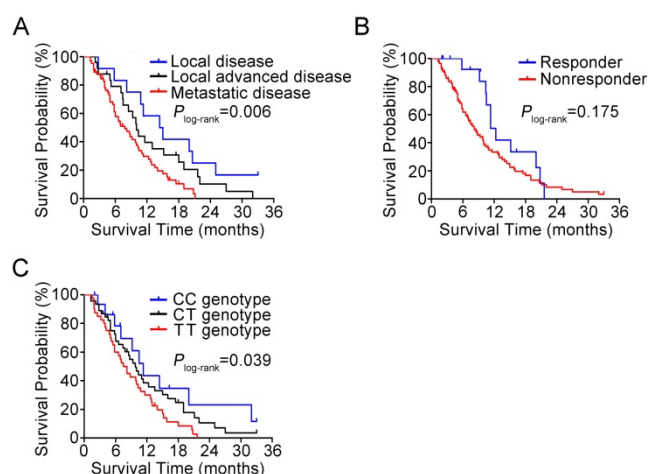


Figure 7. Kaplan-Meier estimation of PDAC survival time in 102 patients. (A) Survival curves by disease stage. **(B)** Survival curves by response to gemcitabine therapy. **(C)** Survival curves by *BACH1* 3'UTR rs372883 genotypes.

BACH1 is broadly expressed in various human tissues [15–17]; however, little was previously known about its role in the development of PDAC. Because *BACH1* is a transcriptional repressor negatively regulating several genes involved in oxidative stress response, cell cycle progression and apoptosis [29], it is reasonable to assume that as a potential tumor suppressor, *BACH1* might act through some of these pathways. Indeed, by gene expression profile analysis using mRNAs from PDAC cells with or without *BACH1* knockdown, we found the significant expression changes in several pathways, including those involved in cell proliferation. Previous study has reported that *BACH1* may inhibit proliferation and angiogenesis of HUVECs through suppressing Wnt/ β -catenin signaling pathway [35]. Other groups have also shown that *BACH1* regulates proliferation of smooth muscle cells during inflammation and atherogenesis [36] and proliferation of murine embryonic fibroblasts in premature cellular senescence of these cells [37]. It has been reported that knockdown of *BACH1* represses the growth inhibitory function of *CXCR3-B* in breast cancer cells [38]. On the other hand, it has been shown that overexpression of miR-155, which can target *BACH1* mRNA, promotes proliferation of renal cancer cells [39]. All these findings indicate that *BACH1* may regulate cell proliferation. Since *HMOX1* (HO-1) is the main target of *BACH1* and is important in the induction of tumorigenic signaling pathways [23, 40–43], in this study we focused on examination of the effects of altered *BACH1* expression on HO-1 and its downstream signaling modules. We demonstrated that in PDAC cells, *BACH1* indeed negatively regulates HO-1 expression. Knockdown of *BACH1* expression substantially increased production of

HO-1 and activation of AKT, ERK and eNOS and elevated *HIF1A* and *VEGF* but decreased *PTEN* expression, which consequentially enhanced cell proliferation ability. In contrast, overexpression of *BACH1* in PDAC cells had reversed effects. Furthermore, the effects of *BACH1* overexpression or knockdown could be rescued when HO-1 was concurrently overexpressed or knocked down in PDAC cells. During this process, we found that *NRF2*, the transactivator of *HMOX1*, may modulate the expression of *HMOX1* by competitive binding to *BACH1*. Taken together, these results indicate that the acting mechanism of *BACH1* in the risk of developing PDAC may at least partially depend on HO-1. In addition, we found that *BACH1* could regulate the expression of genes involved in EMT and stemness, which might also contribute to tumor progression and drug resistance.

It has been well known that some microRNAs may induce mRNA cleavage or suppress translation by binding to the 3'UTR of target mRNA and therefore function as negative regulators of gene expression [44]. In the present study, we show for the first time that *BACH1* expression is regulated by miR-1257 and the rs372883T>C variation diminishes this regulation. Since *BACH1* may function as a tumor suppressor, one may expect that higher constitutional activity of *BACH1* would confer lower risk of cancer formation, which may explain why individuals with the rs372883C allele have reduced PDAC risk compared with those with the rs372883T allele [11]. In line with this notion, we detected higher levels of miR-1257 in PDAC tissues compared with their adjacent normal tissues, implicating an oncogenic role of miR-1257 in PDAC. Since miR-1257 has poorly been investigated in malignancies, our results warrant further studies to examine the regulation and oncogenic role of this microRNA in the formation of PDAC and other types of human cancer.

Another interesting finding in the present study is the correlation between *BACH1* expression levels and response to gemcitabine chemotherapy and survival time in individuals with PDAC. We found that individuals with the rs372883CC genotype had a stronger response to gemcitabine and longer MST compared with those with the rs372883TT genotype, suggesting that rs372883 genotype has potential to serve as a biomarker for identification or prediction of responsiveness to gemcitabine treatment and prognosis of the disease. These clinical findings can be replicated by in vitro drug sensitivity assays in PDAC cells with overexpression or knockdown of *BACH1* and with different *BACH1* rs372883 genotypes in the presence of *BACH1* expression suppressor miR-1257. The association between *BACH1* genotype and

response to gemcitabine and survival time in patients may reflect the function of HO-1 since previous studies have linked HO-1 overexpression to resistance against gemcitabine in pancreatic cancer cells [45, 46]. Nonetheless, we found that HO-1 can rescue only part of the *BACH1* effect, suggesting that there might be other effectors regulated by *BACH1* involved in gemcitabine sensitivity. Indeed, we also found that the expression levels of *ABCC2*, *MGST1* and *NQO1*, which may be downstream of *BACH1*, also had an effect on gemcitabine sensitivity to some degree. On the other hand, we found that the alteration of EMT- and stemness-associated genes may also play an important role in gemcitabine treatment. A more high-throughput study will be helpful to reveal other potential players. Because of the unavailability of target tissue specimens from most PDAC patients in the clinic, *BACH1* rs372883 genotype would be a good surrogate for prediction if this effect can be further validated in a larger size of sample. However, we failed to find such a predictive effect for the rs372883CT genotype, which might be due to mixed expressing alleles of *BACH1* in this group of the heterozygous genotype.

In conclusion, by a set of functional analyses in this study, we demonstrated that rs372883T>C change diminishes the interaction of *BACH1* mRNA 3'UTR with miR-1257, resulting in a high expression of *BACH1* that may more efficiently repress HO-1 expression and consequent oncogenic signaling. These results may explain why rs372883C allele is associated with reduced risk for the development of PDAC as discovered in our previous GWAS in Chinese population. Furthermore, we found that rs372883 genotype is also associated with response to gemcitabine treatment and survival time in patients with PDAC, suggesting that rs372883 genotypes might serve as a biomarker for prediction of gemcitabine treatment efficacy and prognosis of the malignancy.

Abbreviations

AKT: AKT serine/threonine kinase; *BACH1*: BTB and CNC homology 1 gene; ChIP: chromatin immunoprecipitation; ERK: extracellular signal-regulated kinase; ELISA: enzyme-linked immunosorbent assay; EMT: epithelial-mesenchymal transition; GWAS: genome-wide association study; GO: gene ontology; GSEA: gene set enrichment analysis; *HMOX1*: heme oxygenase 1 gene; HUVEC: human umbilical vein endothelial cell; MST: median survival time; PDAC: pancreatic ductal adenocarcinoma; TCGA: the cancer genome atlas; 3'UTR: 3'-untranslated region.

Acknowledgements

This study was supported by National Nature Science Foundation of China (grant number 81572793 to D.L., 81772586 to J.Z. and 81602461 to J.Z.); National High-Tech Research and Development Program of China (grant number 2013CB910302 to C.W.); Natural Science Foundation of Guangdong Province (grant number 2016A030313283 to J.Z.); the Recruitment Program of Global Youth Experts to C.W. and Chinese Academy of Medical Sciences Intramural Funds to C.W. and X.H.

Contributions

D.L., Chen W. and Chengfeng W. conceptualized and supervised this study. X.H., J.Z., J.L. and Xu C. designed and performed functional experiments and data analysis. Wenle T., M.S., Xinxin C., Z.D., Y.Z. and Wen T. performed sample preparation, genotyping assays and association analysis. Chengfeng W. and Xu C. provided clinical samples and data of patients. D.L., X.H. and Chen W. were involved in manuscript preparation. All authors reviewed the manuscript.

Supplementary Material

Supplementary figures and tables.

<http://www.thno.org/v08p3366s1.pdf>

Competing Interests

The authors have declared that no competing interest exists.

References

- Li D, Xie K, Wolff R, Abbruzzese JL. Pancreatic cancer. *Lancet*. 2004; 363: 1049–57.
- Siegel R, Ma J, Zou Z, Jemal A. Cancer statistics, 2014. *CA Cancer J Clin*. 2014; 64: 9–29.
- Burris 3rd HA, Moore MJ, Andersen J, Green MR, Rothenberg ML, Modiano MR, et al. Improvements in survival and clinical benefit with gemcitabine as first-line therapy for patients with advanced pancreas cancer: a randomized trial. *J Clin Oncol*. 1997; 15: 2403–13.
- Oettle H, Richards D, Ramanathan RK, van Laethem JL, Peeters M, Fuchs M, et al. A phase III trial of pemetrexed plus gemcitabine versus gemcitabine in patients with unresectable or metastatic pancreatic cancer. *Ann Oncol*. 2005; 16: 1639–45.
- Raimondi S, Maisonneuve P, Lowenfels AB. Epidemiology of pancreatic cancer: an overview. *Nat Rev Gastroenterol Hepatol*. 2009; 6: 699–708.
- Farrell JJ, Elsalem H, Garcia M, Lai R, Ammar A, Regine WF, et al. Human equilibrative nucleoside transporter 1 levels predict response to gemcitabine in patients with pancreatic cancer. *Gastroenterology*. 2009; 136: 187–95.
- Shi C, Hruban RH, Klein AP. Familial pancreatic cancer. *Arch Pathol Lab Med*. 2009; 133: 365–74.
- Amundadottir L, Kraft P, Stolzenberg-Solomon RZ, Fuchs CS, Petersen GM, Arslan AA, et al. Genome-wide association study identifies variants in the ABO locus associated with susceptibility to pancreatic cancer. *Nat Genet*. 2009; 41: 986–90.
- Petersen GM, Amundadottir L, Fuchs CS, Kraft P, Stolzenberg-Solomon RZ, Jacobs KB, et al. A genome-wide association study identifies pancreatic cancer susceptibility loci on chromosomes 13q22.1, 1q32.1 and 5p15.33. *Nat Genet*. 2010; 42: 224–8.
- Low SK, Kuchiba A, Zembutsu H, Saito A, Takahashi A, Kubo M, et al. Genome-wide association study of pancreatic cancer in Japanese population. *PLoS One*. 2010; 5: e11824.
- Wu C, Miao X, Huang L, Che X, Jiang G, Yu D, et al. Genome-wide association study identifies five loci associated with susceptibility to pancreatic cancer in Chinese populations. *Nat Genet*. 2012; 44: 62–6.

12. Wolpin BM, Rizzato C, Kraft P, Kooperberg C, Petersen GM, Wang Z, et al. Genome-wide association study identifies multiple susceptibility loci for pancreatic cancer. *Nat Genet.* 2014; 46: 994–1000.
13. Childs EJ, Mocci E, Campa D, Bracci PM, Gallinger S, Goggins M, et al. Common variation at 2p13.3, 3q29, 7p13 and 17q25.1 associated with susceptibility to pancreatic cancer. *Nat Genet.* 2015; 47: 911–6.
14. Manolio TA. Bringing genome-wide association findings into clinical use. *Nat Rev Genet.* 2013; 14: 549–58.
15. Igarashi K, Sun J. The heme-Bach1 pathway in the regulation of oxidative stress response and erythroid differentiation. *Antioxid Redox Signal.* 2006; 8: 107–18.
16. Okada S, Muto A, Ogawa E, Nakanome A, Katoh Y, Ikawa S, et al. Bach1-dependent and -independent regulation of heme oxygenase-1 in keratinocytes. *J Biol Chem.* 2010; 285: 23581–9.
17. Sun J, Hoshino H, Takaku K, Nakajima O, Muto A, Suzuki H, et al. Hemoprotein Bach1 regulates enhancer availability of heme oxygenase-1 gene. *EMBO J.* 2002; 21: 5216–24.
18. Vile GF, Basu-Modak S, Waltner C, Tyrrell RM. Heme oxygenase 1 mediates an adaptive response to oxidative stress in human skin fibroblasts. *Proc Natl Acad Sci USA.* 1994; 91: 2607–10.
19. Abraham NG, Kappas A. Pharmacological and clinical aspects of heme oxygenase. *Pharmacol Rev.* 2008; 60: 79–127.
20. Jais A, Einwallner E, Sharif O, Gossens K, Lu TT, Soyol SM, et al. Heme oxygenase-1 drives metaflammation and insulin resistance in mouse and man. *Cell.* 2014; 158: 25–40.
21. Was H, Cichon T, Smolarczyk R, Rudnicka D, Stopa M, Chevalier C, et al. Overexpression of heme oxygenase-1 in murine melanoma: increased proliferation and viability of tumor cells, decreased survival of mice. *Am J Pathol.* 2006; 169: 2181–98.
22. Liu ZM, Chen GG, Ng EK, Leung WK, Sung JJ, Chung SC. Upregulation of heme oxygenase-1 and p21 confers resistance to apoptosis in human gastric cancer cells. *Oncogene.* 2004; 23: 503–13.
23. Sunamura M, Duda DG, Ghattas MH, Lozonoschi L, Motoi F, Yamauchi J, et al. Heme oxygenase-1 accelerates tumor angiogenesis of human pancreatic cancer. *Angiogenesis.* 2003; 6: 15–24.
24. Therasse P, Arbut SG, Eisenhauer EA, Wanders J, Kaplan RS, Rubinstein L, et al. New guidelines to evaluate the response to treatment in solid tumors. European Organization for Research and Treatment of Cancer, National Cancer Institute of the United States, National Cancer Institute of Canada. *J Natl Cancer Inst.* 2000; 92: 205–16.
25. Reichard JF, Sartor MA, Puga A. BACH1 is a specific repressor of HMOX1 that is inactivated by arsenite. *J Biol Chem.* 2008; 283: 22363–70.
26. Hussong M, Borno ST, Kerick M, Wunderlich A, Franz A, Sultmann H, et al. The bromodomain protein BRD4 regulates the KEAP1/NRF2-dependent oxidative stress response. *Cell Death Dis.* 2014; 5: e1195.
27. Pei H, Li L, Fridley BL, Jenkins GD, Kalari KR, Lingle W, et al. FKBP51 affects cancer cell response to chemotherapy by negatively regulating Akt. *Cancer Cell.* 2009; 16: 259–66.
28. Badea L, Herlea V, Dima SO, Dumitrascu T, Popescu I. Combined gene expression analysis of whole-tissue and microdissected pancreatic ductal adenocarcinoma identifies genes specifically overexpressed in tumor epithelia. *Hepatogastroenterology.* 2008; 55: 2016–27.
29. Warnatz HJ, Schmidt D, Manke T, Piccini I, Sultan M, Borodina T, et al. The BTB and CNC homology 1 (BACH1) target genes are involved in the oxidative stress response and in control of the cell cycle. *J Biol Chem.* 2011; 286: 23521–32.
30. Ma J, Sawai H, Ochi N, Matsuo Y, Xu D, Yasuda A, et al. PTEN regulates angiogenesis through PI3K/Akt/VEGF signaling pathway in human pancreatic cancer cells. *Mol Cell Biochem.* 2009; 331: 161–71.
31. Lim KH, Ancrile BB, Kashatus DF, Counter CM. Tumour maintenance is mediated by eNOS. *Nature.* 2008; 452: 646–9.
32. Mai J, Qiu Q, Lin YQ, Luo NS, Zhang HF, Wen ZZ, et al. Angiotensin II-derived reactive oxygen species promote angiogenesis in human late endothelial progenitor cells through heme oxygenase-1 via ERK1/2 and AKT/PI3K pathways. *Inflammation.* 2014; 37: 858–70.
33. Keith B, Johnson RS, Simon MC. HIF1alpha and HIF2alpha: sibling rivalry in hypoxic tumour growth and progression. *Nat Rev Cancer.* 2011; 12: 9–22.
34. Morin RD, O'Connor MD, Griffith M, Kuchenbauer F, Delaney A, Prabhu AL, et al. Application of massively parallel sequencing to microRNA profiling and discovery in human embryonic stem cells. *Genome Res.* 2008; 18: 610–21.
35. Jiang L, Yin M, Wei X, Liu J, Wang X, Niu C, et al. Bach1 represses Wnt/beta-catenin signaling and angiogenesis. *Circ Res.* 2015; 117: 364–75.
36. Omura S, Suzuki H, Toyofuku M, Ozono R, Kohno N, Igarashi K. Effects of genetic ablation of bach1 upon smooth muscle cell proliferation and atherosclerosis after cuff injury. *Genes Cells.* 2005; 10: 277–85.
37. Dohi Y, Ikura T, Hoshikawa Y, Katoh Y, Ota K, Nakanome A, et al. Bach1 inhibits oxidative stress-induced cellular senescence by impeding p53 function on chromatin. *Nat Struct Mol Biol.* 2008; 15: 1246–54.
38. Balan M, Pal S. A novel CXCR3-B chemokine receptor-induced growth-inhibitory signal in cancer cells is mediated through the regulation of Bach-1 protein and Nrf2 protein nuclear translocation. *J Biol Chem.* 2014; 289: 3126–37.
39. Li S, Chen T, Zhong Z, Wang Y, Li Y, Zhao X. microRNA-155 silencing inhibits proliferation and migration and induces apoptosis by upregulating BACH1 in renal cancer cells. *Mol Med Rep.* 2012; 5: 949–54.
40. Zhu X, Fan WG, Li DP, Lin MC, Kung H. Heme oxygenase-1 system and gastrointestinal tumors. *World J Gastroenterol.* 2010; 16: 2633–7.
41. Was H, Dulak J, Jozkowicz A. Heme oxygenase-1 in tumor biology and therapy. *Curr Drug Targets.* 2010; 11: 1551–70.
42. Na HK, Surh YJ. Oncogenic potential of Nrf2 and its principal target protein heme oxygenase-1. *Free Radic Biol Med.* 2014; 67: 353–65.
43. Dennerly PA. Signaling function of heme oxygenase proteins. *Antioxid Redox Signal.* 2014; 20: 1743–53.
44. Bartel DP. MicroRNAs: target recognition and regulatory functions. *Cell.* 2009; 136: 215–33.
45. Berberat PO, Dambrauskas Z, Gulbinas A, Giese T, Giese N, Kunzli B, et al. Inhibition of heme oxygenase-1 increases responsiveness of pancreatic cancer cells to anticancer treatment. *Clin Cancer Res.* 2005; 11: 3790–8.
46. Nuhn P, Kunzli BM, Hennig R, Mitkus T, Ramanauskas T, Nobiling R, et al. Heme oxygenase-1 and its metabolites affect pancreatic tumor growth in vivo. *Mol Cancer.* 2009; 8: 37.